Biosensors and Bioelectronics 24 (2008) 313–318

Contents lists available at ScienceDirect

Biosensors and Bioelectronics

journal homepage: www.elsevier.com/locate/bios

An interleukin-6 ZnO/SiO_2/Si surface acoustic wave biosensor

Soumya Krishnamoorthy[a], Agis A. Iliadis[a,b,*], Thaleia Bei[c], George P. Chrousos[d,e]

[a] Department of Electrical and Computer Engineering, University of Maryland, College Park, MD 20742, USA
[b] Department of Information and Communication Systems Engineering, University of the Aegean, Greece
[c] Section of Endocrinology and Genetics, Developmental Endocrinology Branch, National Institute of Child Health and Human Development, NIH, Bethesda, MD 20892, USA
[d] Section on Pediatric Endocrinology, Reproductive and Molecular Biology Branch, NIH, Bethesda, MD 20892, USA
[e] First Department of Pediatrics, School of Medicine, University of Athens, Athens, Greece

ARTICLE INFO

Article history:
Received 10 January 2008
Received in revised form 19 March 2008
Accepted 3 April 2008
Available online 20 April 2008

Keywords:
Interleukin-6
ZnO
SAW biosensor
Protein immobilization
SiO_2/Si

ABSTRACT

A novel high sensitivity ZnO/SiO_2/Si Love mode surface acoustic wave (SAW) biosensor for the detection of interleukin-6 (IL-6), is reported. The biosensors operating at 747.7 MHz and 1.586 GHz were functionalized by immobilizing the monoclonal IL-6 antibody onto the ZnO biosensor surface both through direct surface adsorption and through covalent binding on gluteraldehyde. The morphology of the IL-6 antibody-protein complex was studied using scanning electron microscopy (SEM), and the mass of the IL-6 protein immobilized on the surface was measured from the frequency shift of the SAW resonator biosensor. The biosensor was shown to have extended linearity, which was observed to improve with higher sensor frequency and for IL-6 immobilization through the monoclonal antibody. Preliminary results of biosensor measurements of low levels of IL-6 in normal human serum are reported. The biosensor can be fully integrated with CMOS Si chips and developed as a portable real time detection system for the interleukin family of proteins in human serum.

1. Introduction

Interleukin-6 (IL-6) is a variably glycosylated secreted glycoprotein and its production is generally correlated with cell activation (Barton, 1997). Circulating IL-6 can be found in the blood of normal individuals in the 1–10 pg/ml and modest elevation is associated with a spectrum of stress and age-related conditions including cardiovascular disease, osteoporosis, arthritis, type 2 diabetes, certain cancers, periodontal disease, frailty, and functional decline (Kiecolt-Glaser et al., 2003). It was also shown that sleep deprivation leads to daytime hyper secretion of IL-6, as well as elevated IL-6 levels were observed in polycystic ovary syndrome independently of obesity or sleep apnea (Vgontzas and Chrousos, 2002; Vgontzas et al., 2006a,b). Hence, effective detection of IL-6 provides an opportunity to develop a better understanding of these conditions, and allows for continuous detection with real-time patient evaluation, thus making it our protein of choice for immobilization and detection studies and the development of novel biosensors. The need for real-time detection of biological and biochemical analytes is a major driving force behind the development of novel biosensor technology (Su and Yanbin, 2004; Berkenpas et al., 2006; Hun and Zhang, 2007). Traditional methods in use for detection of proteins involve standard clinical microbiological assays. These methods generally entail sample collection and incubation at a centralized laboratory where apparatus and expertise are necessary for performing such tests, and cannot safely measure in the low pg/ml ranges.

The aim here is to develop a highly sensitive surface acoustic wave (SAW) biosensor targeting low levels of the interleukin protein family and other proteins. SAW devices are mass transducers that can be miniaturized and integrated into portable micro-array systems. Of the different types of SAW devices, guided shear horizontal (or Love mode) SAW (SH-SAW) devices offer the potential of increased detection sensitivity due to the guided nature of the surface waves (Du et al., 1997; Freudenberg et al., 2001; Berkenpas et al., 2006). SH-SAW devices using quartz (Harding et al., 1997; Howe and Harding, 2000) and $LiTaO_3$ (Gizeli et al., 2003; Guo et al., 2005) have been employed as immunosensors for protein detection, yet SH-SAW sensors on quartz suffer from low electromechanical coupling coefficients, high penetration depth, and low dielectric permittivity with respect to liquid media. SH-SAW devices on $LiTaO_3$ suffer from the attenuation of the acoustic wave due to the excitation of bulk acoustic waves (BAW) in the crystal. ZnO with its large electromechanical coupling coefficient,

* Corresponding author at: Department of Electrical and Computer Engineering, University of Maryland, College Park, MD 20742 USA, Tel.: +1 301 405 3651; fax: +1 301 314 9281.
E-mail addresses: agis@eng.umd.edu, agismd@yahoo.com (A.A. Iliadis).

0956-5663/$ – see front matter © 2008 Elsevier B.V. All rights reserved.
doi:10.1016/j.bios.2008.04.011

strong piezoelectric nature, along with its high affinity for binding biomaterials (Krishnamoorthy et al., 2006), has the potential to offer a novel template for protein immobilization, and ZnO/quartz and bulk immunosensors have been reported with good results (Kalantar-Zadeh et al., 2003; Gabl et al., 2004). When ZnO in epitaxial thin film form is developed on SiO_2/Si substrates, it offers the advantage of monolithic integration with the advanced CMOS technology for peripheral readout and signal processing circuitry. Despite its promise, ZnO thin film growth that is *c*-axis oriented wurtzite crystal structure on the cubic Si substrates, is a challenging task. Yet, high quality ZnO *c*-axis oriented thin films suitable for device development were reported grown on Si and SiO_2/Si substrates by pulsed laser deposition (Krishnamoorthy and Iliadis, 2006b), providing a new material template for sensor development and protein detection.

This work reports the development and evaluation of a ZnO/SiO_2/Si thin film Love mode SAW biosensor prototype capable of detecting low levels of IL-6.

2. Experimental details

2.1. Sensor fabrication

The SAW sensor devices were fabricated by photolithographic processing on ZnO thin films grown on SiO_2/Si. The ZnO thin films were grown by pulsed laser deposition (PLD) on a 500 Å thick SiO_2 layer that was grown on a (1 0 0) Si substrate by dry oxidation in an atmospheric furnace at 1025 °C, as described previously (Krishnamoorthy and Iliadis, 2006b). The pulsed laser ablation system for the ZnO deposition consisted of a KrF laser at a wavelength of 248 nm, operating with an energy density of 0.7 J/cm^2 at a frequency of 10 Hz. The growth temperature and oxygen partial pressure during growth were 250 °C and 1×10^{-4} Torr, respectively. These were optimal growth conditions that resulted in high quality *c*-axis oriented ZnO thin films on the SiO_2/Si substrate.

Two sets of sensor devices were fabricated and compared. Devices A and B were designed targeting a resonant frequency of operation of 0.7 and 1.5 GHz, respectively. The devices were guided shear horizontal (or Love mode) surface acoustic wave (SH-SAW) devices with the ZnO film being the guiding layer of the acoustic wave and the SiO_2 film the substrate. In this type of Love mode device the displacement of the acoustic wave is in-plane the ZnO film guiding layer rather than perpendicular to the film surface, which produces the Rayleigh mode of propagation. Device A was of the inter-digitated transducer (IDT) type, with input and output IDT metallizations made by depositing 500 Å of Al by e-beam evaporation. 500 Å thick Al reflector plates were also deposited on either side of the IDTs, as shown schematically in Scheme 1. The device is designed to be a resonator with finger width and spacing of 1 μm and 2.4 μm, respectively. Device B was designed for the higher frequency of operation with a finger width and spacing of 0.8 μm each. The number of fingers in the input and output IDTs was 15. The length of the IDTs was 45 μm with an aperture of 40 μm for both devices. Al metallization pads were patterned at the input and output IDTs to allow direct on-chip 50 Ω matched microwave probe measurements of the frequency of the sensor devices. A HP8510C parametric network analyzer was used to measure the s-parameters of the SAW sensor devices in the frequency range between 0.3 and 3 GHz.

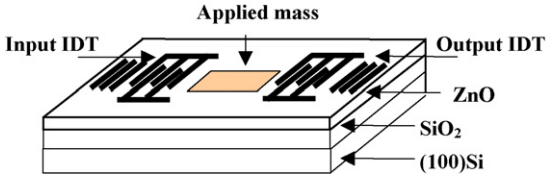

Scheme 1. Schematic representation of the SAW biosensor device showing the active window between the input and output interdigitated transducers (IDTs) for protein immobilization.

The mass sensitivity of the biosensors is calculated as the frequency shift per unit area of applied mass. Our previous study showed that the mass sensitivity of the devices depended on the thickness of the ZnO guiding layer grown on a 500 Å thick SiO_2 layer (Krishnamoorthy and Iliadis, 2006a,b). Maximum mass sensitivity was obtained for ZnO film thicknesses of 340 nm for device A and 136 nm for device B, and these were the optimized ZnO thicknesses used in this work. Furthermore, for accurate measurement of the protein mass, well-defined square windows were opened in the photoresist between the input and output IDTs using standard photolithography. The windows were sized at 5 μm × 5μm and 20 μm × 20 μm and represented the active area of the biosensor devices. The photolithographic procedure was also followed in order to determine the mass sensitivity of the sensors using a well-characterized diblock copolymer for mass measurements. The polystyrene-polyacrylic acid copolymer is well-characterized with a density of 1.077 g/cc (Ali et al., 2006), and was developed in a solvent of tetra-hydro-fluoride (THF) for spin cast application on the sensors. After the windows were opened, the copolymer was spin cast on the sample surface and was allowed to settle before the photoresist was lifted-off in order to form the 5 μm × 5μm and 20 μm × 20 μm windows consisting of the copolymer film only. The copolymer thickness was measured using a Tencor Instruments Alpha-Step 500 profilometer. The thickness measurements showed that a uniform copolymer height was maintained after photoresist removal. The mass deposited on each window area was calculated as the product of the window area, the measured height and the known density of the copolymer. The frequency response of the sensors was measured with and without copolymer mass loading and the mass sensitivity was determined. For device A mass sensitivity was determined to be 4.162 and 4.456 μm^2/pg, and for device B, 8.687 and 8.559 μm^2/pg, for the 5 μm × 5 μm and 20 μm × 20 μm windows, respectively. For these devices the resonant frequency of operation without mass loading was measured to be 747.7 MHz for device A, and 1.586 GHz for device B, in close agreement with the targeted frequencies of 0.7 and 1.5 GHz. All devices were measured and evaluated under constant temperature (22 °C in a class 100 clean room environment) to avoid fluctuations due to temperature variations (Du et al., 1996).

The biosensor devices were used to measure the IL-6 protein mass and study the effectiveness of the IL-6 protein attachment processes. The attachment processes were by (a) direct surface adsorption of the monoclonal antibody and subsequent IL-6 attachment, (b) surface activation and IL-6 immobilization through bovine serum albumin (BSA), and (c) surface activation and IL-6 immobilization through the monoclonal antibody.

2.1.1. Direct surface adsorption

In order to fully evaluate the protein attachment process, the IL-6 antibody was directly adsorbed onto the ZnO sensor window surface and then the IL-6 protein was bound to the antibody (process (a)). This allowed the observation of the morphology of the antibody and IL-6 protein in the absence of any surface activation and treatment, and provided a comparison with the surface activation and protein immobilization processes. The samples were incubated in 1 ml of 1 μg/ml of antibody diluted in 10 mM PBS for 6 h at 4 °C. Different concentrations of IL-6 protein (20, 50, 200, and 500 ng/ml, 1 and 2 μg/ml) were diluted in a 0.1 mg/ml BSA solu-

tion in 10 mM PBS, the samples were incubated for 2 h at 4 °C, then rinsed in 10 mM of PBS, rinsed in ultra pure water, and dried in N_2 gas. The morphology of the adsorbed antibody and IL-6 protein was studied and the mass was quantified by the resonant frequency shift of the biosensor at each stage.

2.1.2. Surface activation and immobilization process

Immobilization of the IL-6 protein on the surface of the ZnO sensor windows can be achieved by activating the surface with hydroxylation, followed by silanization with 3-aminopropyltriethoxysilane (ATES), used as the bridge to which gluteraldehyde is bound, as we have previously reported (Krishnamoorthy et al., 2006). This surface activation developed for the ZnO surface, allows the BSA (Sigma–Aldrich) to covalently bind to gluteraldehyde and IL-6 to bind electrostatically to BSA. In the present work, the process is developed to immobilize the monoclonal antibody, by omitting the BSA step and attaching the antibody covalently directly to gluteraldehyde. The IL-6 protein can then bind to the immobilized antibody to provide a stable and protein specific system.

The ZnO surface silanization process proceeds by the application of 3-aminopropyltriethoxysilane (ATES 99%, Aldrich) solution: (95% aqueous solution of ethanol = 4:100 by volume) at room temperature for 4–5 h. The ATES was applied by low temperature vapor priming (Kumagai et al., 2005). The silanized devices were then rinsed by sonication in ethanol for 1–2 min, washed many times with ultra pure water and baked 10–15 min at 110 °C.

The silanized samples were then immersed in a 2 ml of 2% gluteraldehyde solution (Grade I, 70% Sigma) in 10 mM sodium phosphate-buffered saline (PBS) at pH 7.4, and shaken for 12 h at 4 °C. The samples were then washed thoroughly in ultra pure water to remove the excess gluteraldehyde, and then dried in N_2 gas, before scanning electron microscopy (SEM) examination.

For the immobilization of the IL-6 in the sensor windows through BSA (process (b)), the concentration of BSA was adjusted to 0.1 mg/ml with 10 mM PBS, and 1–2 ml of BSA in PBS solution was incubated shaking for 12–18 h at 4 °C. The samples were rinsed several times in 10 mM of PBS, rinsed in ultra pure water, and dried in N_2 gas (Krishnamoorthy et al., 2006). To monitor the increase in IL-6 mass measured by the biosensor, different concentrations of IL-6 protein ranging from 20 ng/ml to 2 μg/ml (20, 50, 200, 500 ng/ml, 1 and 2 μg/ml) were diluted in 0.1 mg/ml BSA solution in 10 mM PBS, incubated on the sensor windows for 12 to 18 h at 4 °C, and followed by the same rigorous protocol of rinsing and drying.

For the immobilization of the IL-6 protein through the IL-6 monoclonal antibody (process (c)), the sensor window surface was activated up to the gluteraldehyde step, and the monoclonal IL-6 antibody (monoclonal recombinant human-*E. coli* derived IL-6 antibody-500 μg, R&D System, Minneapolis MN, 55413), was immobilized in a covalent binding with gluteraldehyde. The IL-6 protein was then immobilized on the IL-6 antibody. The antibody concentration of 1 μg/ml was diluted in 10 mM PBS and incubated in a shaker for 6 h at 4 °C. The samples were then rinsed several times in 10 mM of PBS, rinsed several times in ultra pure water, and dried in N_2 gas. Different concentrations of IL-6 protein (20, 50, 200, 500 ng/ml, 1 and 2 μg/ml) were diluted in a 0.1 mg/ml BSA solution in 10 mM PBS and the samples with the IL-6 monoclonal antibody were incubated in a shaker for 2–6 h at 4 °C, followed by the same rigorous protocol of rinsing in PBS, pure water, and drying. With the antibody and IL-6 immobilized onto the window of a series of sensors, the resonant frequency shift was measured and the protein mass evaluated.

2.1.3. IL-6 detection in human serum

The biosensors were then used to detect IL-6 protein in human serum (Innovative Research, Southfield, MI, 48034). Two types of

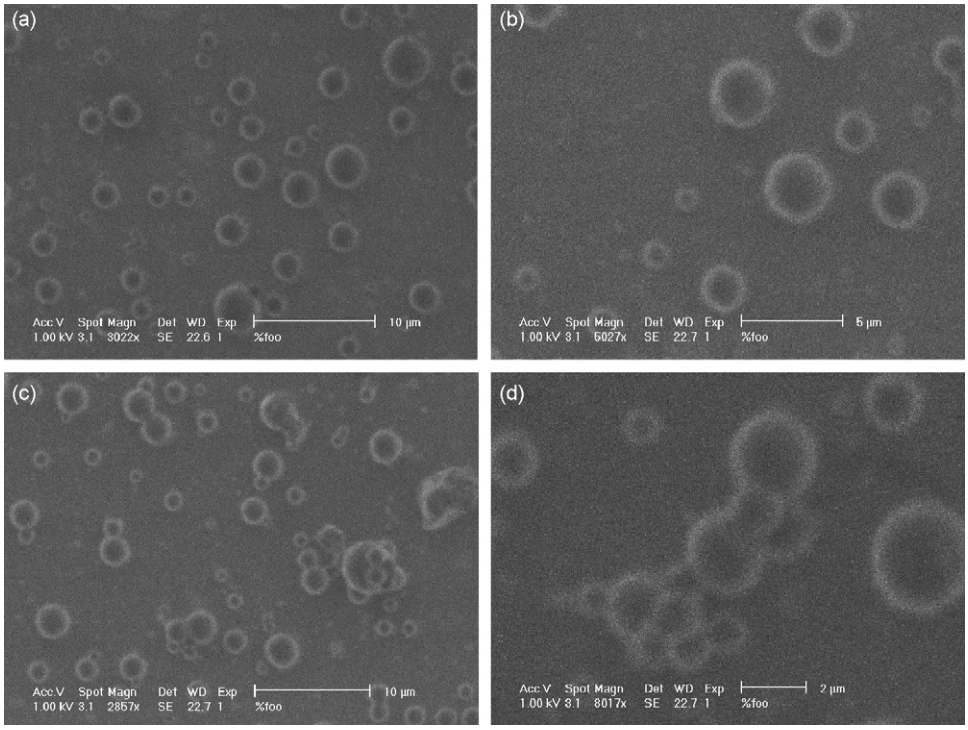

Fig. 1. SEM images of antibody-protein taken during direct surface adsorption. (a) SEM image of antibody adsorbed directly on ZnO surface. Spherical morphology is observed. Antibody particles show darker contrast surrounded by a brighter rim. (b) Same area at higher magnification. (c) The SEM image upon attachment of IL-6 onto the antibody. Spherical morphology and clustering of IL-6 with the antibody is observed. The darker contrast with the brighter rim appearance is evident here also. (d) Same area at a higher magnification.

serum were used in our analysis. Serum A consisted of pooled human serum from multiple donors below the age of 55 (IPLA-SER1) and serum B consisted of normal human serum from a single female donor over 55 years of age (IPLA-SER6). Serum B is expected to contain a higher IL-6 level due to age related conditions. A 250 μl assay dilutent consisting of a buffered protein base with preservative is first added to each sample (RD1D assay dilutent-6 ml, R&D System, Minneapolis MN, 55413). This enhances the binding of IL-6 protein in the human serum to the IL-6 antibody, while inhibiting the attachment of other proteins present in human serum to the antibody. Then, 1 ml of the serum is added and the sensors are incubated as before, washed 10 times with 2 ml of PBS with a 5–10 min soak time provided in the PBS solution between each of the washes, then washed in ultra pure water several times and dried with N_2 gas, before the protein was measured by the resonant frequency shift of the sensor.

3. Results and discussion

3.1. Morphology

Prior to any protein immobilization the fabricated SH-SAW sensor devices were inspected in the SEM to evaluate the exposed ZnO surface in the window openings. The exposed surfaces were found to be morphologically featureless and clean.

3.1.1. Surface adsorption morphology

First the IL-6 antibody was directly adsorbed on the ZnO surface and inspected in the SEM as shown in Fig. 1. Fig. 1(a) and (b) shows the SEM images of the IL-6 antibody bound onto the ZnO surface in low and high magnifications. The antibody particles appear to be distinctly spherical in shape exhibiting a bright rim encircling a darker interior. The lateral size distribution of the particles is ranging between 0.5 and 3 μm. When the IL-6 protein is applied, as seen in Fig. 1(c) and (d), it binds with the antibody forming pairs and clusters extending the lateral dimension to approximately 6 μm. Some antibody particles are observed to remain unpaired. The IL-6 protein is also composed of spherical particles with a darker interior surrounded by a brighter rim.

3.1.2. Surface activation and immobilization morphology

Next, the ZnO surface was activated as described previously for the immobilization process. During the immobilization process, the terminal aldehyde group in gluteraldehyde binds to the amine group of the antibody. This method avoids non-specific attachment directly to the solid phase (Ruhn et al., 1994).

The SEM images of the IL-6 protein immobilization process through the antibody on the exposed ZnO surface at each stage are shown in Fig. 2. Fig. 2(a) shows the SEM image after gluteraldehyde is bound onto ATES. Typical lateral size distribution of these coagulated particles is 1–4 μm throughout the window, as larger area surveys of the ZnO surface have shown. The particles appear to have a lighter contrast and irregular appearance without the darker center or brighter rim seen in the IL-6 antibody-protein morphology.

Fig. 2(b) shows the SEM image when the IL-6 antibody is bound covalently onto gluteraldehyde. The antibody tends to cluster around gluteraldehyde, where the lighter contrast particles in the SEM image represent gluteraldehyde without antibody attachment, while the darker contrast particles with a brighter rim and the more rounded appearance represent the IL-6 antibody attached to gluteraldehyde. This is consistent with the morphology obtained when the antibody is directly adsorbed onto the ZnO surface without the influence of the gluteraldehyde, as seen in Fig. 1(a) and (b).

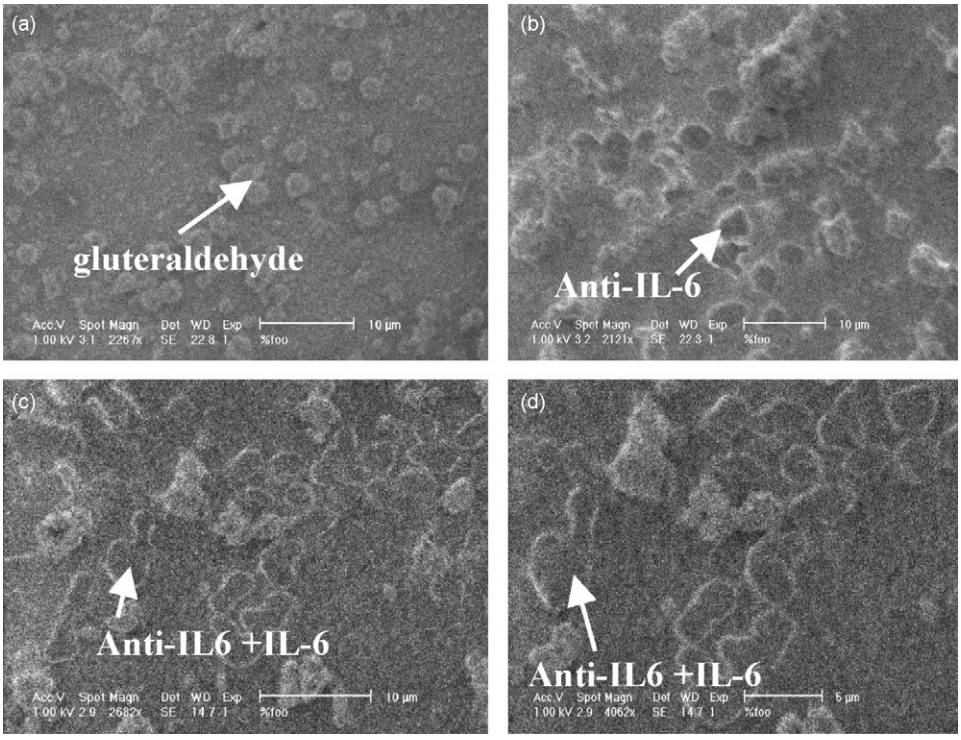

Fig. 2. SEM images of antibody-protein taken during surface activation and immobilization. (a) The SEM image upon application of ATES followed by gluteraldehyde. The morphology indicates coagulated particles of ATES and gluteraldehyde (lighter contrast particles). (b) SEM image upon application of the IL-6 antibody indicates clustering of the antibody (darker contrast particles with brighter rim) attached to gluteraldehyde. (c) SEM image upon application of IL-6 onto the antibody indicates further clustering of IL-6 with the antibody in larger darker contrast rounded clusters. (d) Larger magnification of the same area where the clustering of IL-6 and the IL-6 antibody in darker contrast with brighter rim particles, is evident.

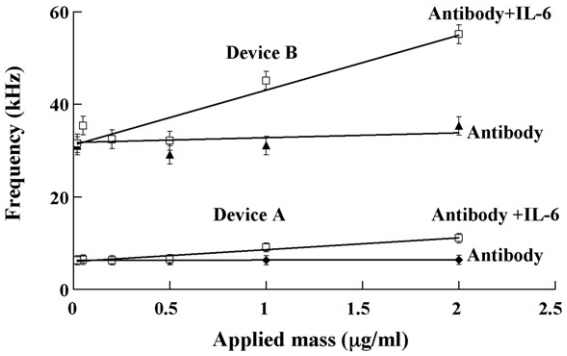

Fig. 3. Direct surface adsorption of antibody and IL-6 protein. Frequency shift with adsorbed antibody and IL-6 mass for biosensor device A operating at center frequency of 747.7 MHz and B operating at 1.586 GHz for an active area window of 5 μm × 5 μm. The higher frequency device B provides significantly larger frequency shifts as compared with the lower frequency device A.

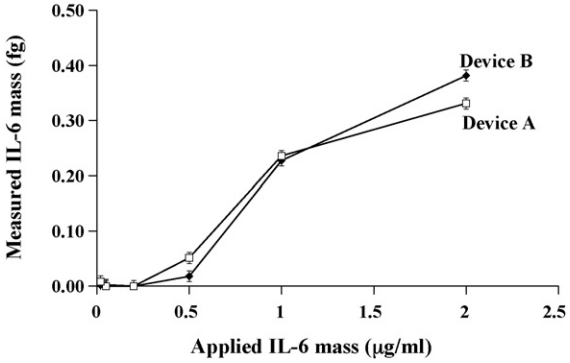

Fig. 4. Direct surface adsorption of antibody and IL-6 protein. From the frequency shifts of Fig. 3 and the known sensitivity of the devices, we derive the measured IL-6 mass versus applied IL-6 mass on the same sensor devices A and B in the 5 μm × 5 μm window.

Lateral size distribution of the antibody is observed to be between 2 and 5 μm.

Fig. 2(c) shows the SEM image after the binding of IL-6 onto the antibody. IL-6 binds with the antibody generating cluster formations in smooth rounded shapes, having a brighter rim surrounding a darker interior, which is consistent with the morphology observed in Fig. 1(c) and (d), for the directly adsorbed antibody-protein clusters.

3.2. Biosensor measurements

Prior to protein immobilization on the windows, the biosensor frequency response was measured to accurately establish the "unloaded" resonant frequency of the device (f_0). The unloaded resonant frequencies obtained were 747.7 MHz and 1.586 GHz for sensor device A and B, respectively, which were consistent with the targeted frequency range of operation intended by the device design. Protein immobilization was then evaluated by measuring the "loaded" frequency of the biosensors and subtracting from the f_0 to extract the mass of the protein.

3.2.1. Direct surface adsorption measurements

For the measurements of the antibody adsorbed directly onto the sensor window (process (a)), the sensors were incubated in 1 ml of 1 μg/ml of antibody diluted in 10 mM PBS for 6 h at 4 °C. A series of sensors were incubated in the same antibody solution and the antibody "loaded" resonant frequency (f_1) was measured, giving a frequency shift ($f_0 - f_1$) of 6.7 kHz and 21.55 kHz (±5%) for a 5 μm × 5 μm window and sensor devices A and B, respectively. In the next step the different concentrations of the IL-6 protein (20 ng/ml–2 μg/ml) were applied on the antibody-loaded sensors, and the frequency spectrum was measured (f_2), to evaluate the attachment process of the protein to the adsorbed antibody.

Fig. 3 shows the frequency shift ($f_1 - f_2$) generated due to the attachment of the IL-6 protein to the antibody in the 5 μm × 5 μm window of devices A and B. Measurements are taken at a constant temperature of 22 °C. From the measured frequency shift and the known sensitivity of the sensors, the mass deposited in the window is determined.

Fig. 4 shows the measured mass of IL-6 protein on the sensor window area for sensor device A and B. A mass of 0.33 and 0.37 fg is measured for an applied IL-6 protein mass of 2 μg/ml for device A and B, respectively. The measured mass appears to have a non-linear relationship, where only trace amounts are detected for applied IL-6 concentrations less than 500 ng/ml. The mass is measurable only when the applied IL-6 protein concentration exceeds 500 ng/ml indicating a weak attachment processes, and suggesting that simple antibody adsorption is not an efficient mechanism for protein attachment and detection. Although the adsorption process allows only limited quantities of the protein to be attached, the sensor can measure levels at sub-fg ranges (Fig. 4(b)).

3.2.2. IL-6 immobilization through BSA

Following the adsorption experiments, the IL-6 protein was immobilized in the sensor window through BSA (attachment process (b)), and the frequency spectra were obtained. The frequency was measured after the application of ATES, gluteraldehyde, and BSA (f_3). Hence, this mass can be obtained from the frequency shift of $f_0 - f_3$.

The different concentrations of IL-6 protein (20 ng/ml–2 μg/ml) were applied and the frequency of the sensors was measured (f_4), to provide the IL-6 mass ($f_3 - f_4$). Fig. 5 shows the IL-6 mass measured as a function of IL-6 mass applied for device B. For device B, the measured IL-6 mass for an applied IL-6 mass of 2 μg/ml in the 5 μm × 5μm and 20 μm × 20 μm windows is 3.01 fg and 24.04 fg, respectively. The surface activation using ATES and gluteraldehyde as intermediary agents to which BSA or the antibody can be bound, helps increase the amount of IL-6 mass bound to the sensor window substantially. The measured IL-6 mass shows a linear relationship with applied IL-6 mass, especially for the high frequency device B. However, for the lower frequency device A (figure not shown), a deviation from linearity in the 20 μm × 20 μm window was observed, indicating possible non-specific attachments to the sensor.

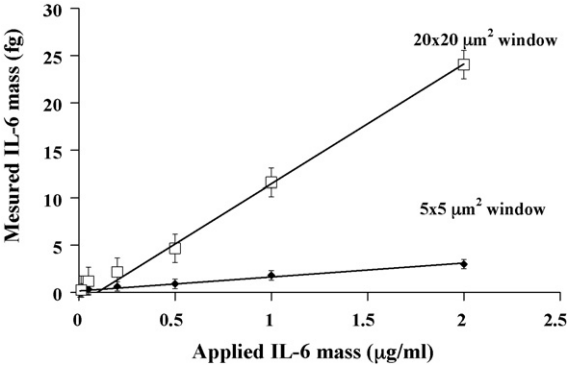

Fig. 5. IL-6 immobilized through BSA. Measured IL-6 mass versus applied IL-6 mass in both 5 μm × 5μm and 20 μm × 20 μm windows for device B operating at a center frequency of 1.586 GHz. Maximum mass detected in a 20 μm × 20 μm window is 24.06 fg for an applied IL-6 mass of 2 μg/ml.

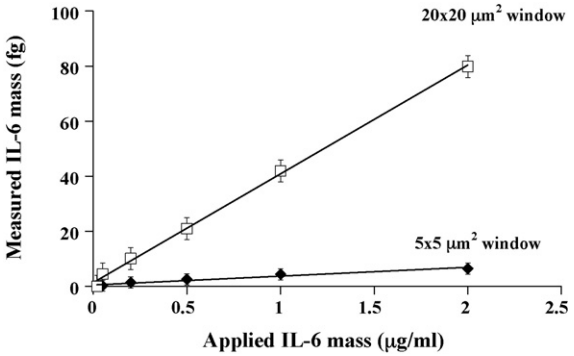

Fig. 6. Specific IL-6 binding through the monoclonal antibody. Measured IL-6 mass versus applied IL-6 mass for specific binding through the IL-6 antibody immobilization process in the 5 μm × 5μm and 20 μm × 20 μm windows for device B. Device B operating at the higher center frequency of 1.586 GHz, shows excellent linearity for both window sizes.

3.2.3. Antibody immobilization and protein measurements

For the immobilization of IL-6 through the antibody, the IL-6 antibody was covalently bound to gluteraldehyde in the sensor windows, and the frequency spectra of the sensors were measured (f_5). The different concentrations of IL-6 protein (20 ng/ml–2 μg/ml) were applied in both windows and the frequency of operation of the devices was measured (f_6), and the IL-6 mass determined from the frequency shift ($f_5 - f_6$). Fig. 6 shows the IL-6 mass measured on device B for both windows. As observed in Fig. 6, the measured IL-6 mass has a linear relationship with applied IL-6 protein. For the high frequency device B the linearity of the data for both window sizes is excellent. For the lower frequency device A, the data for the larger window deviate somewhat from linearity which is consistent also with what is observed in device A for protein attachment through BSA. This suggests that higher frequency and higher sensitivity devices can provide better linearity for protein measurements. Furthermore, a comparison of the immobilization process with the adsorption process indicates an order of magnitude lower protein attachment through adsorption suggesting that adsorbed attachments play no significant role in the detection process. Our results also suggest that increasing active window area can extend the detection range of the sensor to lower concentration ranges, and, combined with the higher frequency and sensitivity, extend the linear range of the sensor to detect substantially lower concentrations of IL-6 mass.

3.2.4. IL-6 protein measurements in human serum

The biosensor activated with the monoclonal IL-6 antibody was used to detect the presence of IL-6 in human serum. The biosensor consisted of device A with a 20 μm × 20 μm window. Human serum A, which consists of pooled human serum from multiple donors under the age of 55, was first applied onto the biosensor and measurements of the frequency in duplicate yielded an average mass of IL-6 protein of 2.27 fg. Serum B, which is from a single female donor above 55 years of age, yielded an average mass value of 6.81 fg, which is three times higher than that in serum A, as expected from age related increases in IL-6 levels (Kiecolt-Glaser et al., 2003).

To confirm the expected increase of IL-6 levels in human serum B, an independent ELISA measurement was performed with a Quantikine High Sensitivity Human IL-6 Immunoassay kit (performed by Machaon Diagnostics, Inc., Oakland, CA, 94609). The ELISA results were done in duplicate using the high precision kit. Serum A was measured to be at 6 and 10 pg/ml of IL-6 protein in the two measurements, and fell within the linear range of calibration of the ELISA kit. Serum B was also measured in duplicate, and found to have IL-6 protein concentrations that fell outside the linear range of calibration of the ELISA kit. Hence, the kit provided only minimum values per measurement for this serum, which were >25 pg/ml of IL-6. Although these values provide just a minimum concentration for IL-6 in the serum, they do show the expected trend for higher levels of IL-6 protein in serum B, in agreement with our sensor.

4. Conclusions

The development of a prototype $ZnO/SiO_2/Si$ guided shear horizontal (Love mode) surface acoustic wave (SH-SAW) biosensor for the detection of IL-6 is reported for the first time. The 0.7 and 1.5 GHz biosensor devices have been developed with optimized guiding layer thickness to achieve maximum mass sensitivity. The active area of the biosensor consisted of two different size square windows where the proteins were attached. Comparison between surface adsorption and surface immobilization through BSA and antibody, showed that the surface adsorption is not an effective approach to antibody-protein attachment and detection, implying that adsorbed species play little or no role in the detection process by protein immobilization. Direct visualization of adsorbed and immobilized antibody-protein complexes through SEM studies showed the antibody-protein morphology and the clustering of the protein with the antibody. The biosensor was shown to have extended linearity, which was observed to improve with higher sensor frequency and for the immobilization process through the monoclonal antibody. Preliminary measurements with the biosensor prototype successfully detected low levels of IL-6 protein in human serum.

Acknowledgement

The support of National Science Foundation through grant # ECS0302494 is gratefully acknowledged.

References

Ali, H.A., Iliadis, A.A., Martinez-Miranda, L.J., Lee, U., 2006. Solid State Electron. 50 (6), 1105–1112.
Barton, B.E., 1997. Clin. Immunol. Immunopathol. 85 (10), 16–20.
Berkenpas, E., Millard, P., da Cunha, M.P., 2006. Biosens. Bioelectron. 21 (12), 2255–2262.
Du, J., Harding, G.L., Ogilvy, J.A., Dencher, P.R., Lake, M., 1996. Sens. Actuators A: Phys. 56 (3), 211–219.
Du, J., Harding, G.L., Collings, A.F., Dencher, P.R., 1997. Sens. Actuators A: Phys. 60, 54–61.
Freudenberg, J., Von Schickfus, M., Hunklinger, S., 2001. Sens. Actuators B: Chem. 71, 147–151.
Gabl, R., Feucht, H.-D., Zeininger, H., Eckstein, G., Schreiter, M., Primig, R., Pitzer, D., Wersing, W., 2004. Biosens. Bioelectron. 19, 615–620.
Gizeli, E., Bender, F., Rasmusson, A., Saha, K., Josse, F., Cernosek, R., 2003. Biosens. Bioelectron. 18, 1399–1406.
Guo, X.S., Chen, Y.Q., Yang, X.L., Wang, L.R., 2005. Proceedings of the 2005 IEEE Engineering in Medicine and Biology 27th Annual Conference, pp. 1922–1924.
Harding, G.L., Du, J., Dencher, P.R., Barnett, D., Howe, E., 1997. Sens. Actuators A: Phys. 61 (1–3), 279–286.
Howe, E., Harding, G., 2000. Biosens. Bioelectron. 15 (11–12), 641–649.
Hun, X., Zhang, Z.J., 2007. Biosens. Bioelectron. 22 (11), 2743–2748.
Kalantar-Zadeh, K., Wlodarski, W., Chen, Y.Y., Fry, B.N., Galatsis, K., 2003. Sens. Actuators B: Chem. 91, 143–147.
Kiecolt-Glaser, J.K., Preacher, K.J., MacCallum, R.C., Atkinson, C., Malarkey, W.B., Glaser, R., 2003. Proc. Natl Acad. Sci. USA 100 (15), 9090–9095.
Krishnamoorthy, S., Iliadis, A.A., 2006 February. Proc. IEEE Sens. Appl. Symp., 14–17.
Krishnamoorthy, S., Iliadis, A.A., 2006 June. Solid State Electron. 50 (6), 1113–1118.
Krishnamoorthy, S., Bei, T., Zoumakis, E., Chrousos, G.P., Iliadis, A.A., 2006. Biosens. Bioelectron. 22 (5), 707–714.
Kumagai, S., Yoshii, S., Yamada, K., Fujiwara, I., Matsukawa, N., Yamashita, I., 2005. J. Photopolym. Sci. Technol. 18 (4), 495–500.
Ruhn, P.F., Garver, S., Hage, D.S., 1994. J Chromatogr. A 669 (1–2), 9–19.
Su, X., Yanbin, L., 2004. Biosens. Bioelectron. 19, 563–574.
Vgontzas, A.N., Chrousos, G.P., 2002. Endocrinol. Metab. Clin. N. Am. 31 (1), 15–30.
Vgontzas, A.N., Trakada, G., Bixler, E.O., Lin, H.M., Pejovic, S., Zoumakis, E., Chrousos, G.P., Legro, R.S., 2006a. Metabolism 55 (8), 1076–1082.
Vgontzas, A.N., Bixler, E.O., Chrousos, G.P., 2006b. Ann. N. Y. Acad. Sci. 1083 (November), 329–344.